Available online at www.sciencedirect.com
SCIENCE DIRECT®
Micron 35 (2004) 431–439
micron
www.elsevier.com/locate/micron

Differential-aperture X-ray structural microscopy: a submicron-resolution three-dimensional probe of local microstructure and strain

Wenge Yang[a,*], B.C. Larson[a], J.Z. Tischler[a], G.E. Ice[b], J.D. Budai[a], W. Liu[b]

[a]*Condensed Matter Sciences Division, Oak Ridge National Laboratory, P.O. Box 2008, Oak Ridge, TN 37831, USA*
[b]*Metals and Ceramics Division, Oak Ridge National Laboratory, P.O. Box 2008, Oak Ridge, TN 37831, USA*

Abstract

A recently developed differential-aperture X-ray microscopy (DAXM) technique provides local structure and crystallographic orientation with submicron spatial resolution in three-dimensions; it further provides angular precision of $\sim 0.01^{\circ}$ and local elastic strain with an accuracy of $\sim 1.0 \times 10^{-4}$ using microbeams from high brilliance third generation synchrotron X-ray sources. DAXM is a powerful tool for inter- and intra-granular studies of lattice distortions and lattice rotations on mesoscopic length scales of tenths of microns to hundreds of microns that are largely above the range of traditional electron microscopy probes. Nondestructive, point-to-point, spatially resolved measurements of local lattice orientations in bulk materials provide direct information on geometrically necessary dislocation density distributions through measurements of the lattice curvature in plastically deformed materials. This paper reviews the DAXM measurement technique and discusses recent demonstrations of DAXM capabilities for measurements of microtexture, local elastic strain, and plastic deformation microstructure.

Keywords: X-ray microscopy; Diffraction; Deformation; Microstructure; Strain

1. Introduction

Most solid materials are composed of crystalline grains or combinations of crystalline grains and amorphous material. Microstructural investigations of the grain size, grain shape, intra- and inter-granular misorientation distributions, impurity distributions, residual strains, lattice defects etc. and their evolution in connection with thermal, mechanical, electrical, and chemical processing techniques have long been goals of materials research (Kocks et al., 1998; Demirel et al., 2003). Accordingly, powerful structural microscopy techniques have been developed for detailed investigation of the microstructure and evolution in materials, especially local orientations and strain distributions.

For instance, powerful transmission electron microscopies (TEM) exist for the identification of new phases in very small volumes, observation of deformation microstructure (and even core structures of defects), chemical bonding measurements using selected area diffraction (Shechtman et al., 1984; Yang et al., 1996), diffraction contrast interpolation (Hirsch et al., 1977; Hughes and Hansen, 1997), convergent beam electron diffraction (CBED) (Tanaka et al., 1988; Zou et al., 1998; Wang, 2000), high resolution electron microscopy (Yan et al., 1998), and electron energy loss spectroscopy (EELS) (Egerton, 1996) techniques. Scanning electron microscopy (SEM) probes equipped with electron backscattering diffraction (EBSD) (Adams et al., 1993; Field, 1997) and atomic force microscopy (AFM) (Gerberich et al., 1998) capabilities are well developed techniques for the study of the surface microstructure.

Detailed dislocation densities and configurations, orientation distributions, and surface profiling have been investigated by these microscopies for thin film, sample surfaces, or thin cross-sections. Moreover, serial sectioning capabilities are now available on EBSD systems so that three-dimensional structural information can be obtained by serial removal of $\sim 1-20$ μm layers between measurement scans (Alkemper and Voorhees, 2001). Despite remarkable progress in the science of materials and materials processing, predicting new materials, establishing new pathways to desired microstructures, or specifying of the overall evolution of materials microstructure by first principles theory and computation is not yet possible.

* Corresponding author. Tel.: +630-252-0888; fax: +630-252-0862.
E-mail address: yangw@ornl.gov (W. Yang).

0968-4328/$ - see front matter © 2004 Published by Elsevier Ltd.
doi:10.1016/j.micron.2004.02.004

A substantial obstacle to progress in this area is our inability to fully handle microstructure and evolution on mesoscopic length scales (tenths-hundreds of microns). Although computer simulations and multi-scale modeling computation techniques are becoming increasingly powerful, the mesoscopic length scale cannot be handled with near the degree of success that is possible with finite element techniques on macroscopic continuum scales (Needleman, 2000), nor with the same degree of facility as say molecular dynamics or discrete dislocation dynamics on the atomic scale (Cleri et al., 1997; Zbib and de la Rubia, 2002). This situation has been exacerbated by the lack of experimental measurements with the submicron, three-dimensional spatial resolution needed over the mesoscopic length scales to provide detailed microstructural input for comparison with the computations. Fortunately, the emergence of high-brilliance, 3rd generation synchrotron sources has made possible great strides in X-ray microstructural capabilities that can now address mesoscopic length scales. A powerful, high-energy 3D X-ray diffraction (3DXRD) technique with ~5 μm resolution over millimeters to centimeters has been developed by the RISØ group at the European Synchrotron Radiation Facility (ESRF) (Poulsen and Fu, 2003). The (monochromatic) 3DXRD technique has been applied to a range of deformation and grain growth investigations and the analysis methods have been discussed in detail (Margulies et al., 2001; Offerman et al., 2002; Poulsen and Fu, 2003). In addition, submicron resolution three-dimensional X-ray structural microscopy techniques have been developed for depth ranges of tens of microns to several hundreds of microns using medium energy, white-X-ray microbeams at the Advanced Photon Source (APS) at Argonne National Laboratory (Larson et al., 2002; Cargill, 2002; Yang et al., 2003). Both of these 3D X-ray techniques are nondestructive and provide microstructural information that will complement the higher spatial resolution, but restricted depth range, information available from electron probes.

In this paper, we overview the DAXM probe technique and discuss demonstrations of submicron resolution 3D microstructural capabilities. Inter- and intra-granular orientation distributions in polycrystals, elastic strain tensors in elastically deformed materials, and plastic deformation microstructures under microindents in Cu single crystals are considered.

2. Differential-aperture three-dimensional X-ray microscopy

High brilliance synchrotron X-ray sources and high precision, achromatic, X-ray focusing optics now make it possible to focus polychromatic, hard X-ray beams to submicron sizes (Ice and Larson, 2000). One of the advantages of hard X-rays for microscopy is the penetration depth, which ranges from tens of microns for higher-Z materials to hundreds of microns (or greater) for lower-Z materials such as Al. Another advantage is the ability to make orientation determinations with high angular precision. By combining submicron diameter incident X-ray beams with the DAXM depth profiling technique developed at the APS (Larson et al., 2002), point-to-point nondestructive structure, orientation, and elastic strain tensor measurements can be made in deformed crystalline materials with micron resolution in all three-dimensions with both white and monochromatic synchrotron radiation. This is a fundamental breakthrough for materials science research at mesoscopic length scale. It provides detailed non-destructive structural information for computational modeling and fundamental elasticity/plasticity theory.

The experimental configuration for submicrometre resolution, three-dimensional X-ray microscopy using DAXM technique on the UNI-CAT Sector-34 undulator beamline at the APS is shown in Fig. 1 (Larson et al., 2002; Yang et al., 2003). A polychromatic (white) X-ray beam enters from the right. The monochromator system is designed to pass a white beam directly or to reflect a monochromatic beam from the lower part of the undulator beam (with double (111) Si crystals) onto the Kirkpatric–Baez (K–B) focusing mirrors. The K–B mirrors on the UNICAT beamline were differentially coated to obtain an elliptical (focusing) figure and provide ~0.5 μm diameter X-ray microbeams with an ~0.5 mm depth of field at the sample position (Ice and Larson, 2000).

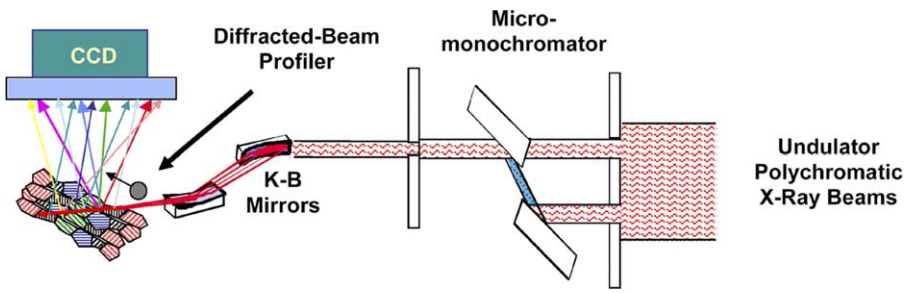

Fig. 1. Schematic depiction of a 3D X-ray structural microscope layout, where the removable/insertable micro-monochromator provides white or monochromatic beams; the elliptically figured K–B mirrors focus the incident beams to ~0.5 μm diameter at the sample position; a 50 μm diameter Pt wire is used as a diffracted beam profiler and a CCD area detector collects white beam Laue diffraction patterns.

The energy range for the current K–B mirrors is 8–25 keV. Unlike the case for TEM, where both reciprocal space (diffraction pattern) and real space (diffraction contrast and high resolution electron microscopy) images can be obtained directly by the use of magnetic lenses, the CCD detector positioned at 90° to the incident beam collects only diffraction patterns in this microdiffraction technique. Since the diffraction patterns from all positions along the penetration depth overlap on the detector, the diffraction patterns contain detailed structural information from an ~0.5 μm diameter line along the microbeam. In order to achieve micron spatial resolution along the penetration direction it is necessary to depth resolve the diffraction patterns for each micron.

Since the diffraction patterns contain ~45° angular cross-fire or larger, profiling the diffraction patterns requires a micron resolution aperture with an angular acceptance of 45° or more. Hard X-ray slits with one micron opening and say ~10 μm thickness for attenuation would pass only about a 6° angular range, so a 50 μm diameter Pt wire is used as a differential-aperture (or knife-edge absorption profiler) to depth resolve the Bragg diffracted intensity from the sample (see Fig. 2). By taking submicron steps of the Pt wire parallel to the sample surface and subtracting diffraction patterns (i.e. CCD images) taken before and after each step, one can obtain the differential intensity distribution that passes through the pinhole-like camera submicron gap between the two wire positions, as depicted in Fig. 2. Computer reassembling of the differential intensity

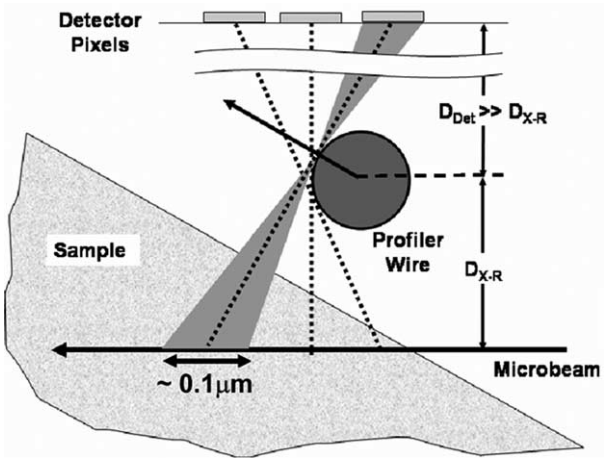

Fig. 2. Schematic view of the differential-aperture profiling geometry. This (not-to-scale) illustration shows the large angular acceptance and the small parallax (~0.1 μm as described in the text) associated with differential-aperture profiling using a circular cross-section highly absorbing wire at a position where $D_{Det} \gg D_{X-R}$. The small parallax (or uncertainty in the source of intensity in each ~20 μm pixel) ensures that the change in intensity in a pixel before and after a one μm step of the wire has a resolution along the microbeam given almost entirely by the step size of the profiling wire. Note that the tangential point of diffracted rays on the wire changes as a function of the angular direction of the diffracted X-rays; this is taken into account in the analysis and makes the large angular acceptance possible with submicron resolution.

distribution for each depth segment along the microbeam is accomplished by collating the differential intensities in each CCD pixel for each step of the profiler. The source of the intensity is then determined by triangulating from the pixel position of the intensity in the CCD to the wire position, and then extrapolating to the beam position to determine the source of intensity along the microbeam. This makes it possible to reconstruct full diffraction patterns for sub-micron voxels along the penetration direction.

From the diffraction patterns, it is possible to obtain complete diffraction information (i.e. structure, orientation, strain tensor, etc.) for each segment of material along the penetration direction of the X-ray microbeam. The pixel positions, the geometrical parallax associated with the ~20 μm pixel size, the profiler step size, the profiler direction, and the circular shape of the Pt wire are all taken into account in the depth analysis. Typically, the wire is stepped along the sample surface, which is 45° from the incident beam. It is necessary for the overall precision and accuracy of the method that the distance from CCD to wire (D_{Det}) is ~200 times larger than that from incident X-ray beam to wire ($D_{X\text{-}R}$). The spreading width along the penetration direction due to the CCD 20 μm pixel size is given by 20 μm × ($D_{X\text{-}R}/D_{Det}$) ≈0.1 μm (see Fig. 2). This condition ensures that the parallax correction due to the CCD pixel size is small, and that the spatial resolution of the reconstructed diffraction patterns is determined primarily by the step size of the Pt wire. Therefore, depth resolution significantly smaller than a micrometer is achievable. Typically, profiler scans are made with one-micron steps along the (45°) sample surface (i.e. 0.7 μm along the beam); for such conditions, computer collation and reconstruction of the differential intensities can be made with resolution of ~0.8 μm considering the 0.1 μm parallax contribution.

The analysis of the depth resolved diffraction patterns so obtained is performed using computer automated techniques developed for crystallographic indexing, orientation extraction, and strain determination developed for single- or multi-layered thin film samples (Chung and Ice, 1999; Tamura et al., 1999; Budai et al., 2003). As outlined in the flow diagram in Fig. 3, the reconstructed digital CCD Laue images are interactively or automatically indexed and analyzed to obtain the structure and orientation as a function of depth. This is handled after precise calibration of the detector position and orientation with respect to the incident beam using a standard Si or Ge (perfect, strain-free) single crystal. The (nominal) lattice parameters of the materials to be investigated are input as known parameters for orientation and deviatoric strain determinations.

Since each depth profiling scan provides information along a single line, three-dimensional structural data are compiled by translating the sample over a lateral array of positions with micron or submicron step sizes. Typically at each sample position, depth profiling scans take 300–400 steps to cover the entire CCD with white beams, which requires 20–30 min. For the case of a scanning

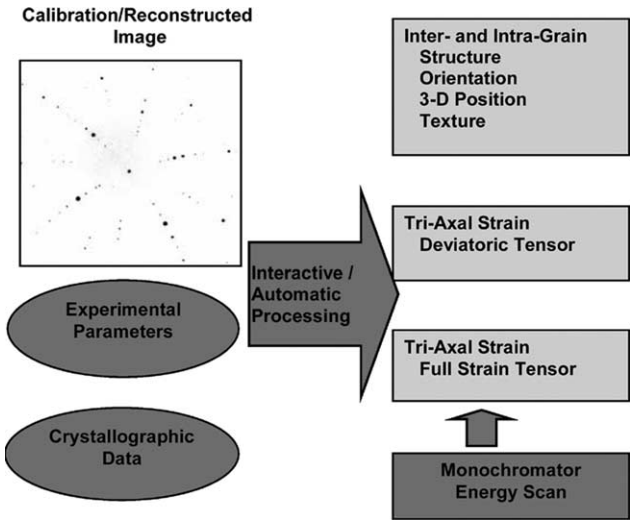

Fig. 3. Flow diagram of the data analysis procedure in which calibration is performed by analyzing the diffraction pattern from a perfect, strain free Si or Ge crystal.

monochromatic beam (Yang et al., 2003), only one Bragg reflection is excited and around 50 steps are needed for a single diffraction peak; this requires ~2–3 min. The scanning speed is limited by the detector readout time in both the white and monochromatic cases. The computer reconstruction and analysis of the depth resolved diffraction patterns for each increment along the beam typically requires ~30 min to index and analyze entire Laue patterns and ~30 s for a single monochromatic diffraction peak on a 2 GHz Pentium 4 computer. Decreasing these times by a factor of 10 or more will be possible by using faster detectors and computer clusters.

3. Applications

3.1. Intra- and inter-granular structure of polycrystalline materials

Thermal-mechanical treatment of metals represents one of the most important industrial processing techniques. Hot-roll processing, for instance, is based on the deformation, nucleation, local crystallographic recovery, and recrystallization of polycrystalline grains by grain-boundary motion to achieve desired grain textures and sizes. While much has been learned about the process from decades of highly refined X-ray texture investigations and from recent surface and serial sectioning EBSD, and, moreover, information on individual grain growth is being provided by high-energy 3DXRD (Offerman et al., 2002) investigations, local intra-and inter-granular evolution investigations with micron point-to-point 3D resolution have not been possible. DAXM now provides the capability to perform nondestructive 3D grain growth measurements by detailed mapping of the polycrystalline structure as a function of sequential thermal annealing steps. Such information is critical for the evaluation of computer simulations of grain growth and other materials processes.

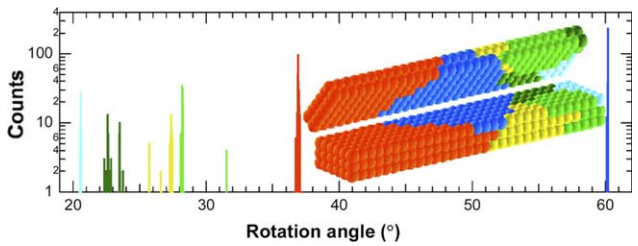

Fig. 4. Histogram of the orientation angles (relative to a lab coordinate system) of each point in a $5 \times 6 \times 31$ μm^3 volume. The inset is the polycrystal microstructure coded with colors defined by the orientation angles. The narrow widths of the individual peaks indicate generally small intra-granular (mosaic) rotation angles for the individual grains even though the dark green and yellow colors include a range of angles for clarity of presentation.

Fig. 4 illustrates a three-dimensional mapping of polycrystalline grain structure using DAXM. The sample measured was a hot rolled (200 °C) polycrystalline Al (1% Fe, Si) alloy. A 5×6 array of DAXM line scans with one micron lateral spacing was measured using the DAXM procedure discussed in Section 2, and grain orientations for 31 μm along the incident beam are displayed in a color coded fashion. In addition to the 3D display of the crystal grains, the figure contains color coded log scale histograms generated using the rotation angles of each 1 μm^3 voxel (relative to the lab coordinate system) in the $5 \times 6 \times 31$ μm^3 volume measured. Since the angular resolution for the orientations is ~0.01°, the sub-structure of each grain is available and plotted with 0.1 degree intervals in the graph in Fig. 4. The single, isolated, sharp peaks for the red and blue grains indicate that there is very little variation in the orientation of these grains over their entire volumes. On the other hand, for the grains coded in yellow and dark green, there exist subgrain structures with ~2° misorientations. Although the ~0.01° angular resolution of the orientation measurements makes it possible to plot grain-boundaries (or rotational plastic strains) with differences of only a few hundredths of a degree, Fig. 4 collects ~2° regions into a single color for clarity of presentation. Making use of the digital, computer coded nature of the data, the top two layers of the display have been rotated up from remaining layers to show the interior grain structure. Similar measurements of deformation induced local lattice rotations have been made near the boundary of a plane-strained Al bi-crystal region using the DAXM technique (Larson et al., 2004). Recognizing the importance of grain-boundaries, grain orientations, grain sizes, and their thermal evolution characteristics in materials processing design and applications, the use of this technique to monitor the intra- and inter-granular evolution of embedded grains in three dimensional bulk materials will provide direct information for simulations and multi-scale modeling to understand microstructural evolution.

3.2. Spatially resolved strain tensor measurements

The impact of externally applied stress distributions and processing or deformation induced residual stresses in materials is of central importance in understanding the performance and microstructural evolution of structural materials Although standard polycrystalline X-ray diffraction methods provide statistical information on residual stresses in materials, computer simulations and modeling directed toward obtaining a detailed understanding of materials on the microscale are in critical need of local intra- and inter-granular stresses/strains. As demonstrated below using the case of cylindrically bent Si, both the local crystal orientation and the local elastic strain tensors can be measured with 3D submicron resolution using white and monochromatic DAXM measurements (Larson et al., 2002; Yang et al., 2003).

As depicted in Fig. 5a, cylindrical bending of brittle materials such as Si produces a uniform elastic strain gradient through the depth of the material. This provides an ideal sample to demonstrate the capability of simultaneously determining the local crystal orientation and elastic strain tensors when both are varying continuously. Such a capability is of course critical for a structural microscopy technique in order to ensure that both rotational strain and elastic strain distributions can be measured, both inter-granularly and intra-granularly. Fig. 5a illustrates schematically that the strain component along the bending direction ε_{xx} is positive at the top and negative at the bottom and continuously changes along the thickness direction. For thin plates (Landau and Lifshitz, 1986), the strain component $\varepsilon_{xx} = t/R$, where t is measured from the center line of the plate and R is the bend radius; for a wide plate the strain along the transverse direction $\varepsilon_{yy} = 0$. We note that the microbeam traverses continually rotating portions of the crystal as it penetrates at an angle into the bent crystal.

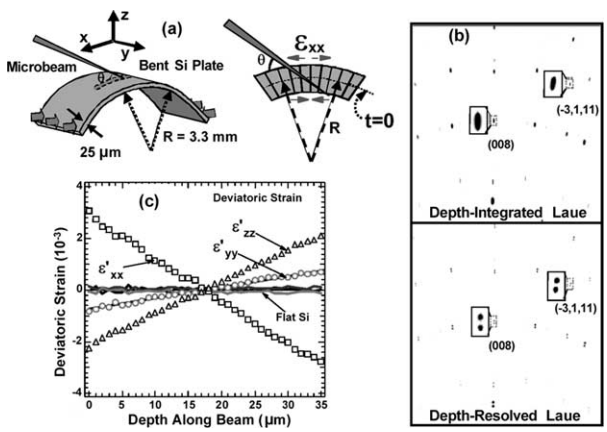

Fig. 5. (a) Schematic view of the geometry for spatially resolved measurement of the orientation and strain tensors in cylindrically bent Si; (b) depth integrated and depth resolved Laue patterns; (c) depth resolved deviatoric strain tensors.

Depth integrated and depth resolved Laue patterns are shown in Fig. 5b. The streaking of the enlarged (008) and (−3 1 11) reflections for the depth integrated pattern clearly shows the lattice rotation. The non-vertical streak of the (−3 1 11) reflection indicates the sensitivity of the Laue pattern to the varying strain state as a function of depth. Neither local orientation nor strain information can be obtained from the depth integrated patterns. However, the depth resolved patterns (given for the top and bottom of the sample) provided by the DAXM technique, and shown in the lower panel, illustrate that DAXM provides full Laue diffraction patterns for each micron along the microbeam. Thus, full crystal orientation and strain tensor analyses can be made on the diffraction patterns from each depth within the sample. The deviatoric (i.e. shear) strain tensor components specifying the shape distortions of the unit cell (Noyan and Cohen, 1987) as a function of depth were obtained directly from the white beam Laue pattern by least-squares analysis of the precise Bragg peak positions, treating the elastic strain tensor components as adjustable parameters. Similar measurements on a flat (unstrained) Si sample yielded the solid lines in Fig. 5c, showing the strain to be zero within the $+/-10^{-4}$ uncertainty of the measurements. The ε'_{xx} components of the deviatoric strain (i.e. along the bend direction) are large and tensile at the top of the Si arch and large and compressive at the lower surface. As expected, the sign of the z-component (i.e. along the surface normal) is opposite to that of ε'_{xx} as a result of Poisson compression (extension) along the surface normal at the top (bottom) surface. These measurements demonstrate that local orientations and local strains can be determined simultaneously, even when both are changing continuously.

White beam Laue diffraction patterns of the form measured in Fig. 5 do not provide information on the absolute lattice parameter (Chung and Ice, 1999). Therefore, in order to obtain the full strain tensor including the dilatation as well as the deviatoric strain, it is necessary to measure at least one d-spacing in absolute terms. Without discussing the details here, a scanning-monochromatic form of DAXM has been developed that provides micron-resolution depth-resolved d-spacings, from which dilatational strain can be determined by comparison with the lattice parameter of unstrained material (Yang et al., 2003). Fig. 6 shows the result of such a monochromatic DAXM measurement on cylindrically bent Si in which the solid line represents the strain gradient expected from the cylindrical bend parameters. Since the scanning-monochromatic form of DAXM requires depth related Bragg energies and Bragg angles for only one reflection at each depth, it can be performed using scanning monochromatic beams. This means that it can be performed using Fresnel zone plates or refractive X-ray lenses on monochromatic beam line without the requirement of white beams and achromatic focusing optics.

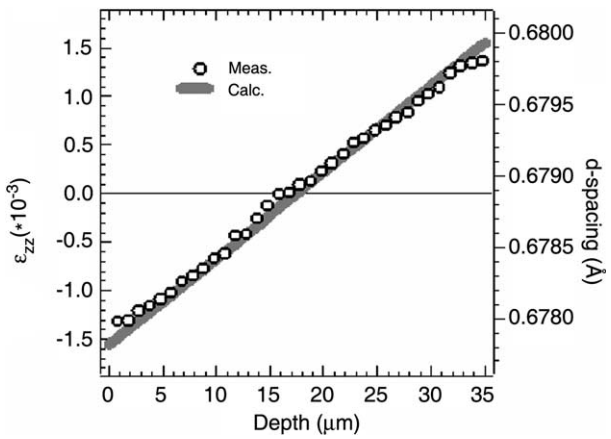

Fig. 6. Depth dependence of lattice spacings and surface normal strain in cylindrically bent Si measured using monochromatic DAXM, open circles; the solid line represents surface normal strains calculated for the cylindrically bent Si.

3.3. Plastic deformation microstructure

Plastic deformation generates, in crystalline materials, complex distributions of dislocations on microscopic and mesoscopic length scales, which are controlled by dislocation interactions and self-arrangement (Hughes and Hansen, 1997; Hansen, 2001). The dislocation distributions required to accommodate the local lattice curvature generated by plastic deformation processes are referred to as geometrically necessary dislocations (GNDs) (Gao and Huang, 2003). Since all dislocations would be considered geometrically necessary if curvature were measured on length scales down to a few lattice spacings, it is necessary to specify the length scale over which curvature is to be measured for the term GND to be meaningful in a quantitative sense. Understanding the spatial resolution of curvature measurements as the length scale provides a practical usage and this convention is used here. Categorizing dislocations as 'necessary' or 'incidental' has been used in TEM studies (Hughes et al., 1997, Hughes et al., 2003); to the extent that no net curvature is associated with the incidental dislocations such a definition is consistent with the usage adopted here. The DAXM capability to determine local lattice orientations with submicron, point-to-point spatial resolution provides direct information on the local lattice curvature in three dimensions; this information provides a quantitative measurement of GND densities in plastically deformed regions with the one-micron spatial resolution of the measurements as the length scale for curvature measurement.

Fig. 7 displays micro-indent induced lattice rotation measurements on a Cu single crystal generated by a 100 mN maximum load Berkovich indent and by a 200 mN maximum load spherical indent with 69 μm radius. The point of entry of the microbeam and its penetration direction are indicated on the optical image of the Berkovich indented surface. The microbeam Laue diffraction pattern generated by the deformed Cu under the Berkovich indent is shown in Fig. 7c. The triangular shaped streak pattern for each (hkl) reflection indicates lattice rotations of several degrees around well-defined crystallographic axes. The enlarged view of the (hhh) reflection in Fig. 7e shows that the intensity along the streaks is uneven; this implies that the rotations along the microbeam penetration depth are not uniform, but rather have regions of small curvature interspersed with large rotations. The presence of a complicated deformation pattern would of course not be surprising for a beam traversing under the sharp blade-edge region between the two faces of the pyramidal indenter.

Local orientations were determined for each micron step along the penetration direction of the beam as presented elsewhere (Yang et al., 2004). The misorientation angle and (nominal) rotation axis from one step along the microbeam penetration depth to the next are plotted in Fig. 7 g. We note again that the rotation axes often seem to change discontinuously with depth for micron resolution measurements. The rotation axes are approximately along the [1 0 −1] direction for the first few micrometers, which corresponds to the direction of rotation imposed by the left face of the Berkovich indenter. As the beam penetrates deeper, there is an abrupt change to rotation along the [3 2 −3] axis, which is followed by rotations around the [1 −2 0] axis. The rotation axis for the deepest material at this measurement line has a [1 −1 0] rotation axis, which corresponds to the rotation imposed by the upper indent blade. In the interest of clarity, the few degrees rotation of the indenter orientation off the sample symmetry direction has been ignored in indicating the approximate rotation axes of the point-to-point misorientations.

For the 200 mN maximum load, spherical indent case, similar depth profiling measurements were made at the off-center position marked in Fig. 7b. Unlike the extremely sharp curvature changes induced by the Berkovich blades, more continuous lattice rotations were found underneath the spherical indent. The arc shaped form of intensity from the Laue pattern in Fig. 7d and the enlarged (hhh) reflection in Fig. 7f indicate that the local lattice rotations are smoother than that for Berkovich case; however, there are also small discontinuities and positions where the axes of rotation change rapidly with depth along the beam penetration direction. The detailed misorientation axes and misorientation angles are plotted in Fig. 7 h. Initially (i.e. near the sample surface) the rotation axis is along the [−4 3 2] direction; the rotation axis then changes to the [−2 −3 4] direction and subsequently to the [−2 −3 0] direction before settling in to the [1 −1 1] direction at deepest distance.

These measurements made for single positions are not sufficient to calculate 3D GND densities; 3D GND densities require lattice orientation measurements made over a lateral area as well as a function of depth. By making a two dimensional array of depth profiler scans around an indented area, one can get the three dimensional

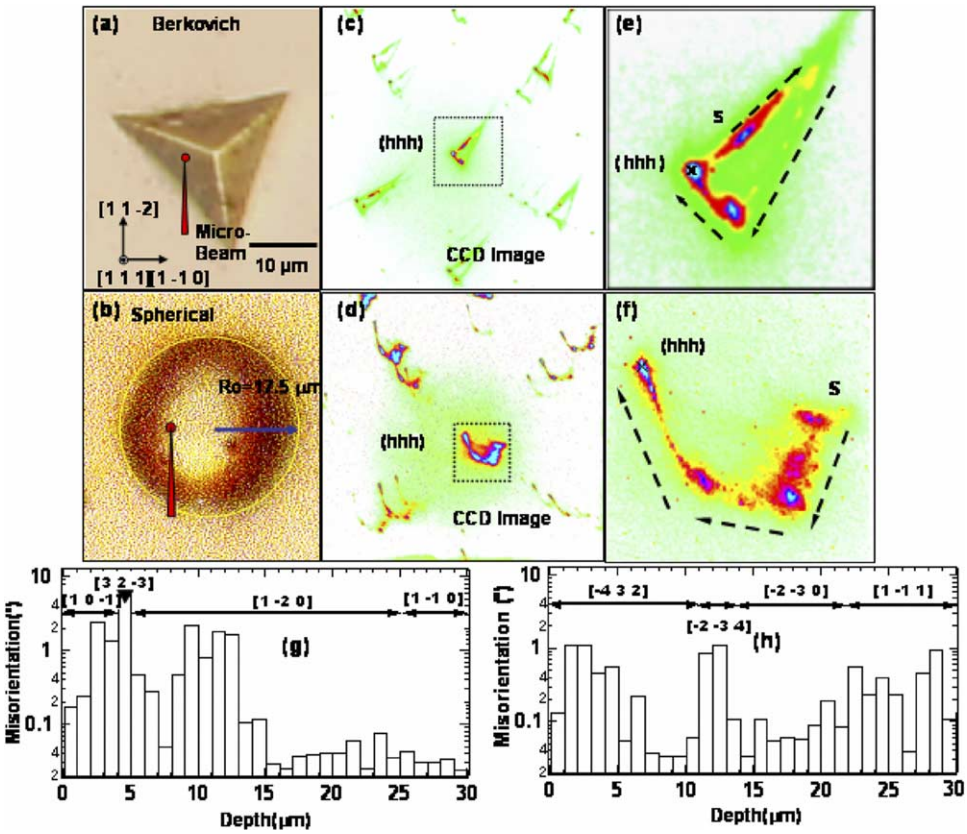

Fig. 7. Plastic deformation microstructure measurements under micro-indents in <111 oriented Cu. Optical images of (a) a 100 mN Berkovich indent and (b) a 200 mN Spherical indent with 69 μm radius; (c), (d) full Laue patterns for Berkovich and Spherical indents, respectively; (e), (f) expanded view of the (hhh) reflection from Berkovich and spherical indents, respectively; ‘×’ in (e) and (f) denotes the undeformed orientation; (g),(h) Log plots of the point-to-point misorientation angles and the point-to-point rotation axes for Berkovich and spherical indents, respectively.

local lattice curvature for the entire deformed volume below the indenter; this procedure is analogous to that used in measuring the polycrystalline grain structure in Fig. 4. Such measurements are presently in progress. Three-dimensional lattice rotation and rotation axis information under nanoindents will provide quantitative measurements of GNDs with ~ one-micron resolution that can be compared directly with detailed simulations and modeling.

The measurement length scale of the DAXM microbeam X-ray microscopy measurements discussed here are complementary to the length scales of electron microscopy measurements of indent deformation. For instance, direct observation of dislocation motion has been made in epitaxial films and substrates through nanoindentation measurements in-situ in a TEM (Minor et al., 2003). Also, a direct comparison has been made between ex situ TEM measurements of the dislocation microstructure under a nanoscale indent of Cu and dislocation dynamics simulation and finite element modeling by Robertson and Fivel (1999). It will be important to connect mesoscale plastic deformation measurements made by DAXM with the micro and nanoscale measurements made by TEM. This will provide deformation microstructure information over a wide range of length scales and be of significant help to computer simulations and multiscale modeling to form a better understanding of fundamental deformation mechanisms.

4. Discussion

The applications discussed in Section 3 relate to three important aspects of materials research:

The point-by-point crystallographic orientation distribution of polycrystalline materials provides three-dimensional microtexture, angular mosaic of grains, grain morphology, and grain-boundary normal directions. The so-called five degrees of freedom (three for the misorientation between the lattices of two interfacing grains and two for the orientation of the boundary plane) for describing grain boundary geometry (Randle, 1992) can be fully determined (nondestructively) by the techniques described here. Serial sectioning with EBSD can provide this information, but it is a destructive method and would not apply for studies of the evolution of microstructure, such as thermal grain growth.

The spatially resolved elastic strain capabilities discussed provide the actual residual stress distribution in real materials. Elastic strain is of course not retained

during thin sectioning for TEM, so this capability is of significant importance. It is expected to be of particular interest for investigations of cracks during brittle fracture and in fatigued samples, and in detailed investigations of polycrystalline materials under stress and plastic deformation.

As discussed, the 3D lattice curvature measurement capability will provide quantitative GND density distributions that can be directly connected to computer simulations of defect microstructure under plastic deformation (El–Azab, 2000).

Modifications and extensions of the technique can be anticipated; these include hardware, software, and analysis developments that will enhance its capabilities as well as extend the range of applications to geological, environmental, biological, structural mechanics and other disciplines, in additional to the materials physics applications addressed here.

5. Summary

An overview of the three-dimensional, nondestructive, submicron-resolution structural microscopy method for submicron resolution measurements of local lattice structure, orientation, and both elastic and plastic distortions has been presented. Measurements of micro-texture and intra- and inter-granular orientations in a polycrystalline Al alloy were presented, depth dependent strain tensor measurements were discussed for an elastically bent Si single crystal, and local lattice curvature measurement from two types of micro-indentation in Cu have been considered. These illustrations demonstrate the capabilities of the DAXM technique for quantitative studies of microstructure and evolution on mesoscopic length scales. The technique is complementary to electron microscopy in that it is a nondestructive method applicable to mesoscopic length scales of tenths of microns to hundreds of microns, whereas TEM has much higher spatial resolution but is restricted to thin section samples. Combined TEM, DAXM, and high-energy 3D X-ray techniques will provide a wide range of length scales over which microstructure and evolution investigations can be applied in connection with advanced computer simulation and modeling to extend fundamental investigations of materials.

Acknowledgements

We thank G.M. Pharr, H. Weiland, K.-S. Chung, N. Tamura, J.-S. Chung, E. Williams, W.P. Low and E. Dufresne for their contributions during this work. The measurements were performed on the MHATT-CAT and UNICAT beam lines at the Advanced Photon Source (APS). This research was supported by the DOE Basic Energy Sciences, Division of Materials Sciences under contract with Oak Ridge National Laboratory, managed by UT-Battelle, LLC. The UNICAT facility at the APS is supported by the US DOE under Award No. DEFG02-91ER45439, through the Frederick Seitz Materials Research Laboratory at the University of Illinois at Urbana-Champaign, the Oak Ridge National Laboratory (US DOE contract DE-AC05-00OR22725 with UT-Battelle LLC), the National Institute of Standards and Technology (US Department of Commerce) and UOP LLC. The APS is supported by the US DOE, Basic Energy Sciences, Office of Science under contract No. W-31-109-ENG-38.

References

Adams, B.L., Wright, S.I., Kunze, K., 1993. Orientation imaging: the emergence of a new microscopy. Metall. Trans. A 24, 819–831.

Alkemper, J., Voorhees, P.W., 2001. Quantitative serial sectioning analysis. J. Microsc. 201, 388–394.

Budai, J.D., Yang, W., Tamura, N., Chung, J.-S., Tischler, J.Z., Larson, B.C., Ice, G.E., Park, C., Norton, D.P., 2003. X-ray microdiffraction study of growth modes and crystallographic tilts in oxide films on metal substrates. Nat. Mater. 2, 487–492.

Cargill, G.S., 2002. Microscopy-extra dimension with X-rays. Nature 415, 844–845.

Chung, J.-S., Ice, G.E., 1999. Automated indexing for texture and strain measurement with broad-band-pass X-ray microbeams. J. Appl. Phys. 86, 5249–5255.

Cleri, F., Yip, S., Wolf, D., Phillpot, S.R., 1997. Atomic-scale mechanism of crack-tip plasticity: dislocation nucleation and crack-tip shielding. Phys. Rev. Lett. 79, 1309–1312.

Demirel, M.C., Kuprat, A.P., George, D.C., Rollett, A.D., 2003. Bridging simulation and experiments in microstructure evolution. Phys. Rev. Lett. 90, 016106.

Egerton, R.F., 1996. Electron energy loss spectroscopy in the electron microscope, 2nd ed, Plenum, New York.

El-Azab, A., 2000. Statistical mechanics treatment of the evolution of dislocation distributions in single crystals. Phys. Rev. B 61, 11956–11966.

Field, D., 1997. Recent advances in the application of orientation imaging. Ultramicroscopy 67, 1–9.

Gao, H., Huang, Y., 2003. Geometrically necessary dislocation and size-dependent plasticity. Script. Mater. 48, 113–118.

Gerberich, W.W., Harvey, S.E., Kramer, D.E., Hoehn, J.W., 1998. Low and high cycle fatigue—A continuum supported by AFM observations. Acta Mater. 46, 5007–5021.

Hansen, N., 2001. New discoveries in deformed metals. Metall. Mater. Trans. A 32, 2917–2935.

Hirsch, P., Howie, A., Nicholson, R.B., Pashley, D., Whelan, M.J., 1977. Electron microscopy of thin crystals, Huntington, New York.

Hughes, D.A., Hansen, N., 1997. High angle boundaries formed by grain subdivision mechanism. Acta Mater. 45, 3871–3886.

Hughes, D.A., Hansen, N., Bammann, D.J., 2003. Geometrically necessary boundaries, incidental dislocation boundaries and geometrically necessary dislocations. Scripta Mater. 48, 147–153.

Hughes, D.A., Liu, Q., Chrzan, D.C., Hansen, N., 1997. Scaling of microstructural parameters: misorientations of deformation induced boundaries. Acta Mater. 45, 105–112.

Ice, G.E., Larson, B.C., 2000. 3D X-ray crystal microscope. Adv. Eng. Mater. 2, 643–646.

Kocks, U.F., Tome, C.N., Wenk, H.R., 1998. Texture and Anisotropy—preferred orientations in polycrystals and their effect on materials properties, Cambridge University Press, Cambridge.

Landau, L.D., Lifshitz, E.M., 1986. Theory of Elasticity, 3rd ed, Pergamon, New York.

Larson, B.C., Yang, W., Ice, G.E., Budai, J.D., Tischler, J.Z., 2002. Three-dimensional X-ray structural microscopy with submicrometre resolution. Nature 415, 887–890.

Larson, B.C., Yang, W., Tischler, J.Z., Ice, G.E., Budai, J.D., Liu, W., Weiland, H., 2004. Micro-resolution 3-D measurement of local orientations near a grain-boundary in plane-strained aluminum using X-ray microbeams. Int. J. Plast. 20, 543–560.

Margulies, L., Winther, G., Poulsen, H.F., 2001. In situ measurement of grain rotation during deformation of polycrystals. Science 292, 2392–2394.

Minor, A.M., Stach, E.A., Morris, J.W. Jr., Petrov, I., 2003. In-site nanoindentation of epitaxial TiN/MgO (001) in a transmission electron microscopy. J. Electron Mater. 32, 1023–1027.

Needleman, A., 2000. Computational mechanics at the mesoscale. Acta Mater. 48, 105–124.

Noyan, I.C., Cohen, J.B., 1987. Residual stress: measurement by diffraction and interpretation, Springer, New York.

Offerman, S.E., van Dijk, N.H., Sietsma, J., Grigull, S., Lauridsen, E.M., Margulies, L., Poulsen, H.F., Rekveldt, M.T., van der Zwaag, S., 2002. Grain nucleation and growth during phase transformations. Science 298, 1003–1005.

Poulsen, H.F., Fu, X., 2003. Generation of grain maps by an algebraic reconstruction technique. J. Appl. Crystallogr. 36, 1062–1268.

Randle, V., 1992. Microtexture determination and its applications, The Institute of Materials, London.

Robertson, C.F., Fivel, M.C., 1999. A Study of the submicron indent-induced plastic deformation. J. Mater. Res. 14, 2251–2258.

Shechtman, D., Blech, I., Gratias, D., Cahn, J.W., 1954. Metallic phase with long-range orientational order and no translational symmetry. Phys. Rev. Lett. 53, 1951–1951.

Tamura, N., Chung, J.-S., Ice, G.E., Larson, B.C., Budai, J.D., Tischler, J.Z., Yoon, M., 1999. Strain and texture in Al-interconnect wires measured by X-ray microbeam diffraction. Mater. Res. Soc. Sym. Proc. 563, 175–180.

Tanaka, M., Terauchi, M., Kaneyama, T., 1998. Convergent-Beam Electron Diffraction II, JEOL Ltd, Tokyo.

Wang, R., 2000. Defocus convergent beam electron diffraction determination of Burgers vectors of dislocations in quasicrystals. Micron 31, 475–486.

Yan, Y., Chisholm, M.F., Duscher, G., Maiti, A., Pennycook, S.J., Pantelides, S.T., 1998. Impirity-induced structural transformation of a MgO grain boundary. Phys. Rev. Lett. 81, 3675–3678.

Yang, W., Gui, J.N., Wang, R., 1996. Some new stable one-dimensional quasicrystals in an $Al_{65}Cu_{20}Fe_{10}Mn_5$ alloy. Phil. Mag. Lett. 74, 357–366.

Yang, W., Larson, B.C., Ice, G.E., Tischler, J.Z., Budai, J.D., Chung, K.S., Lowe, W.P., 2003. Spatially resolved Poisson strain and anticlastic curvature measurements in Si under large deflection bending. Appl. Phys. Lett. 82, 3856–3858.

Yang, W., Larson, B.C., Pharr, G.M., Ice, G.E., Budai, J.D., Tischler, J.Z., Liu, W., 2004. Deformation microstructure under microindents in single-crystal Cu using three-dimensional X-ray structural microscopy. J. Mater. Res. 19, 66–72.

Zbib, H.M., de la Rubia, T.D., 2002. A multiscale model of plasticity. Int. J. Plast. 18, 1133–1363.

Zou, H., Liu, J., Ding, D.-H., Wang, R., Froyen, L., Delaet, L., 1998. Determination of interfacial residual stress field in an $Al–Al_2O_3$ composite using convergent-beam electron diffraction technique. Ultramicroscopy 72, 1–15.